Comparison of the spectrum of a sunspot-like star with a sunspot

J.L. LINSKY[1], T.R. AYRES[2], A. BROWN[2], and R.A. OSTEN[2]

[1] JILA, University of Colorado and NIST, Boulder, CO 80309-0440 USA
[2] CASA, University of Colorado, Boulder, CO 80309-0389

Received 2002 May 10; accepted 2002 July 3

Abstract. A typical sunspot umbra has an effective temperature, gravity, and strong magnetic field strength similar to the dM1e star AU Microscopii. We compare STIS, *Chandra*, *EUVE*, and *FUSE* spectra of AU Mic with typical spectra of sunspots to characterize the major differences and then compare models of AU Mic with sunspot models. We find that the emission, heating rates, and differential emission measure distributions are very different for AU Mic and sunspots, and conclude that the root cause of the difference lies in the very different geometries of the two magnetic fields.

Key words: Sun: sunspots – stars: spots – stars: chromospheres – stars: coronae – ultraviolet emission – X-rays

1. Comparison of physical properties

The umbrae of large sunspots have two important properties – low effective temperature and strong magnetic fields – that suggest that a comparison with an active M dwarf star with similar properties may shed some light on the role that magnetic fields play in the heating and structure of the chromospheres and coronae of both objects. Since the topic of this "thinkshop" is the study of both sunspots and starspots, let's follow the comparison to where it may lead. In particular, we would like to answer the following questions:

(1) Does an active M dwarf star with properties similar to a sunspot umbra have the same UV and X-ray emission as a sunspot umbra and its overlying active region?

(2) How do the chromosphere, transition region, and coronae of AU Mic and the sunspot umbra/active region differ?

(3) What may be the cause of the different atmospheric structures?

We chose AU Microscopii (HD 197481) as our comparison star because it is the most X-ray luminous of the nearby early-M dwarf stars, and there are excellent UV and X-ray spectra available for analysis. Unfortunately, solar spectra do not have comparable spectral resolution, spectral coverage, or signal/noise. Pagano et al. (2000) reported on the nonflare portion of a 10.1 ks STIS E140M spectrum of AU Mic with a resolution of 6.6 km s^{-1} and covering the 1170–1730 Å bandpass. Robinson et al. (2001) reported on the flare portion of this spectrum. Del Zanna, Landini, and Mason (2002) analyzed of the *EUVE* and *FUSE* spectra of AU Mic. Here we discuss our 60 ks *Chandra* HETG/ACIS-S X-ray spectrum of AU Mic obtained on 2000 Nov 12.

Correspondence to: jlinsky@jila.colorado.edu

Table 1 summarizes the physical properties of AU Mic and a typical large sunspot umbra. The AU Mic properties are taken from Pagano et al. (2000). The magnetic field strength (4,200 G) and filling factor (0.55) taken from Saar (1993) are an average over the whole star and likely underestimate the field strength in any starspot that may be present on AU Mic. The magnetic field strength (B_0) for the center of a sunspot umbra is taken from the magnetostatic models of Moon, Yun & Park (1998).

$P_{\rm gas}$ refers to the gas pressure and B_0 refers to the magnetic field at reference height 0 km in the Moon et al. (1998) models, which corresponds to optical depth $\tau = 2/3$ and a Wilson depression 600 km. For AU Mic, $P_{\rm gas}$ is from a solar abundance Kurucz model with $T_{\rm eff} = 3775$ K and $\log g = 4.5$.

The bolometric luminosity (L_{bol}) refers to a hypothetical star with the same effective temperature as the sunspot and the solar radius. The X-ray luminosity (L_x) refers to the Sun when it is most active, i.e., when the maximum number of active regions cover the solar disk (Peres et al. 2000).

For both AU Mic and the sunspot umbra, the magnetic pressure exceeds the gas pressure, $\beta = 8\pi P_{\rm gas}/B_0^2 < 1$, even in the deep photosphere and certainly higher in the atmosphere as the gas pressure scale height is far smaller than the magnetic field scale height. This agreement and the similar effective temperatures and gravities suggest that the sunspot and AU Mic should have similar UV and X-ray emission and spectra. However, as we shall see, this is not the case.

Table 1. Physical Properties of AU Mic and a Large Sunspot

Property	AU Mic	Sunspot
Spectral type	dM1e	K7
$T_{\rm eff}$ (K)	3775	4200 ± 200
Gravity ($g/g_{\odot}$)	1.70	1.00
B_0 (G)	4200	3000
log $P_{\rm gas}$ (dynes cm^{-2})	5.28	5.266
$\beta = 8\pi P_{\rm gas}/B_0^2$	0.27	0.53
$P_{\rm rot}$ (days)	4.865	25.38
log $L_{\rm bol}$ (erg s^{-1})	32.40	33.03
log $L_{\rm X}$ (erg s^{-1})	29.74	28.49
log $L_{\rm X}/L_{\rm bol}$	–2.66	–4.54
log f_X (ergs cm^{-2} s^{-1})	7.41	5.70

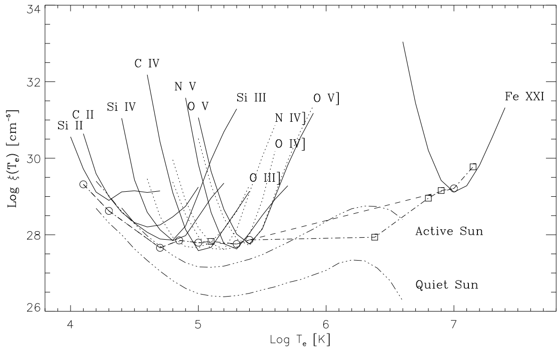

Fig. 1. Emission measure distribution from the analysis of STIS ultraviolet spectra of AU Mic. From Pagano et al. (2000).

2. Comparison of chromospheres and transition regions

Pagano et al. (2000) derived an emission measure distribution from analysis of the nonflare STIS spectrum of AU Mic. In the region $4.5 < \log T < 5.5$, the EM(T) is about 20 times larger than for the quiet Sun and about 5 times larger than for a typical active region. The radiative loss rate from this region of the atmosphere is thus 5 times larger than from a solar active region.

Redshifts of transition region lines of AU Mic are close to 0 km s^{-1} (Redfield et al. 2002a), whereas for the Sun (quiet and active regions) the redshifts are typically +10 km s^{-1}. Thus the flow patterns of the active Sun and AU Mic are very different.

3. Comparison of coronae

3.1. Estimating the X-ray properties of a sunspot/active region

Unfortunately, there are no X-ray observations of the Sun as a point source directly comparable to observations of stars by satellites like *ROSAT*, *ASCA*, *Chandra*, and *XMM-Newton*. To remidy this problem, Peres et al. (2000) have estimated how the Sun at different levels of activity would appear if it

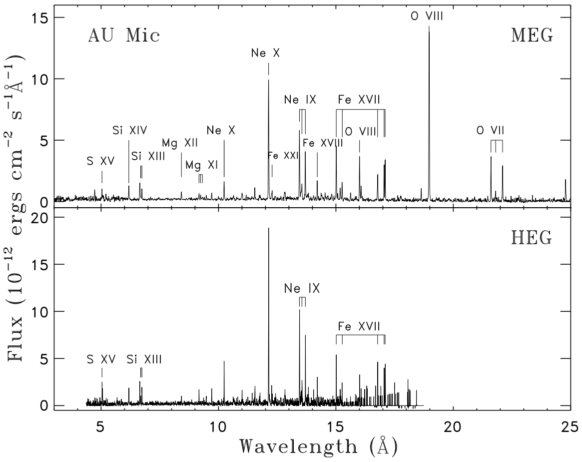

Fig. 2. The *Chandra* spectrum of AU Mic with important emission lines marked. The top panel is the from the Medium Energy Grating (MEG) and the lower panel is from the High Energy Grating (HEG).

were observed as a point source by the PSPC instrument on *ROSAT*. Their analysis is based on broad-band *Yohkoh* X-ray observations of the Sun. Extending their approach, Drake et al. (2000) derived an emission measure distribution and X-ray flux for the brightest active regions (2% of the area of the disk) seen on the Sun at the time of solar maximum. If the whole Sun were completely covered by the most active regions, the X-ray luminosity as seen by *ROSAT* would have been 3.1×10^{28} ergs s^{-1}, comparable to such moderately active stars as ϵ Eri and ξ Boo A, but a factor of 15 less luminous in X-rays than AU Mic.

Table 1 lists the X-ray properties for this hypothetical very active Sun that would probably come closest to simulating the corona above a sunspot. The X-ray surface flux of this "star", and thus roughly the coronal heating rate per unit area, is a factor of 50 smaller than for AU Mic, indicating that AU Mic is not just a scaled up sunspot.

3.2. Analyzing the Chandra data set

AU Mic was observed for 60 ks by the *Chandra* HETG/ACIS on 2000 Nov 12. The resolution varies from 500–1,000 across the 4–25 Å bandpass. The data set contains no large flares, but many small flares are likely present. We calibrated the data using CIAO V.2.1.1 and the procedures listed in the CIAO "threads." The MEG and HEG lightcurves and integrated spectra were determined from the resulting Level 2 events file and PHA file.

The MEG and HEG spectra (see Fig. 2) were analyzed using the iterative measuring process of Osten et al. (2002). We assumed an interstellar hydrogen column density N(H I) = 2.0×10^{18} cm^{-2} obtained from ISM measurements. The fluxes of the strongest unblended emission lines were measured by Gaussian fitting, and the detected Fe lines were then used to determine an initial differential emission measure (DEM) distribution using the APEC (version 1.10) line list and emissivities. We also included Fe XV and Fe XVII line fluxes observed by *EUVE* in 1992 July 14–17 (Monsignori Fossi et al. 1996) to extend the DEM to lower temperatures.

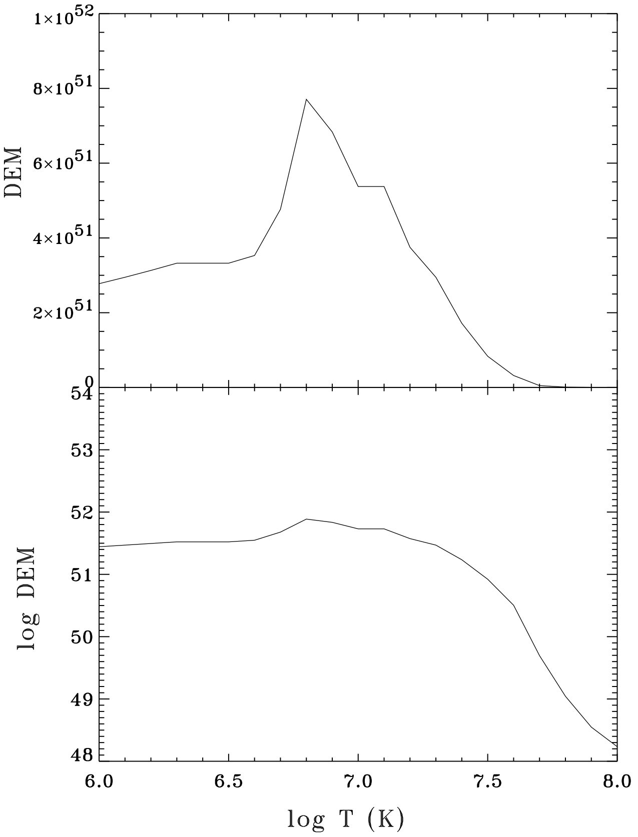

Fig. 3. Differential emission measure distribution obtained from the analysis of *Chandra* X-ray spectra of AU Mic. Top panel is a linear scale and the bottom panel is a log scale.

¿From this DEM distribution we calculated the continuum and fitted it to the line-free regions of the spectrum. The derived continuum was then subtracted from the MEG and HEG spectra and the emission line fluxes remeasured. After three iterations the emission line fluxes and continuum spectrum had converged. The DEM (see Fig. 3) is based on 25 emission lines from *Chandra* (S/N $> 2.5\sigma$) and 2 lines from *EUVE*.

3.3. Results of the differential emission measure analysis

- The DEM peaks at $\log T = 6.8$ in the analysis of the *Chandra* and *EUVE* (Del Zanna et al. 2002) data sets for AU Mic. For solar active regions the peak is at $\log T = 6.5$ (Drake et al. 2000).
- At temperatures below the peak, the DEM is essentially flat (determined by Fe XV, Fe XVI, and Fe XVII) for AU Mic but falls rapidly for the solar active region.
- At temperatures above the peak, the DEM of AU Mic falls less rapidly than for the solar active region.

Thus the shape of the DEM is unlike that of solar active regions and is probably more like solar flares. Also, the corona of AU Mic has no net bulk flow. We know this from the -2.0 ± 2.5 km s^{-1} radial velocity of the Fe XXI λ 1354 line relative to the photosphere (Pagano et al. 2000), and the -5 ± 10 km s^{-1} radial velocity of the Fe XVIII λ977 line (Redfield et al. 2002b). Thus the X-ray emitting plasma is likely confined by strong coronal magnetic fields.

3.4. Coronal abundances

The iron (Fe) abundance in the corona of AU Mic was measured by comparison of the observed continuum with that predicted from the Fe-based emission measure distribution. We found Fe/H to be 0.36 times the solar photospheric abundance (Grevesse & Sauval 1999). The abundances of other elements (see Table 2) were measured relative to Fe from the ratios of observed line fluxes to that predicted by the Fe-based EM distribution. We find that the abundances of metals with first ionization potential (FIP) less than 13.61 eV are underabundant compared to the solar photosphere. The abundances of another active dwarf star AB Dor show a similar pattern. This result is a part of a larger problem that can be summarized as follows:

Table 2. Coronal Abundances Relative to the Solar Photosphere

Abundances	FIP (eV)	AU Mic	AB Dor	Solar AR
Mg/H	7.64	0.22	0.51	
Fe/H	7.87	0.36	0.37	
Si/H	8.15	0.49	0.66	
O/H	13.61	0.42	0.71	
Ne/H	21.56	1.59	1.00	
Fe/Ne		0.23	0.10	0.7–3.0
Fe/O		0.86	0.52	0.74–1.75
O/Ne		0.26	0.71	0.72–1.74

- In solar coronal loops and slow speed wind, metals with FIP < 10 eV are enhanced typically by a factor of 4 relative to the photosphere (the so-called **FIP effect**).
- In solar coronal holes and high speed wind metal abundances are photospheric.
- In the coronae of active stars, metals with FIP < 10 eV are depleted relative to the photosphere, but high-FIP elements (e.g., Ne) can be overabundant (**anti-FIP effect**).
- Metal abundances in solar active regions are hard to measure, but they appear to show a small FIP effect (McKenzie & Feldman 1992).

Thus unlike solar active regions, the metal abundances in the corona of AU Mic are anti-FIP. To our knowledge, there is no available quantitative model to explain the anti-FIP effect.

4. Electron densities

Electron densities are usually derived from ratios of emission lines that have different sensitivities to density due to different collisional or radiative rates. Del Zanna, Landini, and Mason (2002) have demonstrated that even when using lines of the same ion to avoid abundance and ionization differences, other complications such as optical depth, formation over a wide temperature range, and poor atomic data can lead to very uncertain densities. In particular, ions in the lithium and sodium isoelectronic sequences, including such commonly studied ions as C IV, N V, O VI, and Si IV, often provide uncertain emission measures and electron densities.

The C III 977Å/1175Å ratio is commonly used to infer electron densities at transition region temperatures near $T = 6 \times 10^4$ K. *FUSE* observations of α Cen A, a good analog of the quiet Sun, have a C III line flux ratio of 0.361 ± 0.051, corresponding to an electron density, $\log n_e = 9.62 \pm 0.18$ (Redfield et al. 2002a). By comparison, the line ratio for ϵ Eri, a good analog for a solar active region, is 0.658 ± 0.093, and the line ratio for AU Mic is 0.88 ± 0.12. These line ratios likely indicate a sequence of increasing electron density, but Del Zanna et al. (2002) show that this line ratio leads to very uncertain electron densities above 10^{10} cm^{-3}.

Ratios of lines within the O IV multiplet (1399Å, 1401Å, 1404Å, 1407Å) are more reliable diagnostics of electron densities near $T \approx 1.8 \times 10^5$ K. In their analysis of STIS spectra of AU Mic, Pagano et al. (2000) conclude that the 1407Å/1401Å ratio is most reliable, yielding $\log n_e = 10.80 \pm 0.12$. Del Zanna et al. (2002) arrive at nearly the same result $\log n_e = 10.70$–10.95. This corresponds to a transition region pressure $n_e T_e = 1.25 \times 10^{16}$, about 20 times higher than for the quiet Sun.

5. Why are AU Mic and a sunspot umbra/active region different?

The analysis of AU Mic's UV spectrum from STIS, its X-ray spectrum from the *Chandra* HETG, the extreme ultraviolet spectrum from *EUVE*, and the far-UV spectrum from *FUSE* have allowed us to compare the DEM distribution, electron densities, heating rates, flows, and coronal element abundances of the star with a sunspot umbrae and its overlying coronal active region. What have we learned from this comparative study and what explanation is there for the very different emission and heating rates from the star and a sunspot?

- The emission per unit surface area from the transition region of AU Mic is 5 times larger than for a very active region on the Sun, and the coronal emission per unit ares is 50 times larger. Also, the shape of the coronal DEM of AU Mic is very different from a solar active region. The coronal emission of AU Mic is more like a solar flare than an active region (e.g., Güdel 1997; Drake et al. 2000). Thus, despite similar T_{eff}, gravity, and magnetic field strengths, the starspot star is <u>not</u> like sunspots and the active regions above them.
- The local heating rates for AU Mic are larger than for the sunspot by about the same factors, although the amount of energy in the photospheric radiation field and magnetic field is not very different.
- The strong magnetic fields of sunspots are usually isolated, so that the field diverges rapidly. The inclination angle at the sunspot boundary is about 72° (Lites et al. 1993). Observed vertical field gradients are in the range 0.2–several G km^{-1} (Moon et al. 1998). Vertical field divergence for AU Mic must be very small because the filling factor of the magnetic field is very large.
- The more rapidly that magnetic fields diverge with height, the higher that MHD waves will shock in the atmosphere and the larger the cross-sectional area to be heated. The larger area and lower densities mean less heating per unit area and lower UV and X-ray emission in the sunspot compared to AU Mic.
- The buffeting of closely packed strong magnetic fields in AU Mic by convective turbulence should lead to enhanced flare heating in this star compared to the sunspot, where the surrounding magnetic field is weak.

We therefore conclude that it is the very different geometries of the magnetic fields of AU Mic and a sunspot that are the root cause of the very different UV and X-ray emission of these two atmospheres, which have with similar T_{eff}, gravity, and photospheric magnetic field strength.

Acknowledgements. This work is supported by NASA grants S-56500-D and H-04630D to the University of Colorado and NIST.

References

Del Zanna, G., Landini, M., Mason, H.E.: 2002, A&A 385, 968
Drake, J.J., Peres, G., Orlando, S., Laming, J.M., Maggio, A.: 2000, ApJ 545, 1074
Grevesse, N., Sauval, A.J.: 1999, A&A 347, 348
Güdel, M.: 1997, ApJ 480, L121
Lites, B.W., Elmore, D.F., Seagraves, P., Skumanich, A.P.: 1993, ApJ 418, 928
McKenzie, D.L., Feldman, U.: 1992, ApJ 389, 776
Moon, Y.J., Yun, H.S., Park, J.S.: 1998, ApJ 494, 851
Monsignori Fossi, B.C., Landini, M., Del Zanna, G., Bowyer, S.: 1996, ApJ 466, 427
Osten, R.A., Ayres, T.R., Brown, A., Linsky, J.L., Krishnamurthi, A.: 2002, ApJ, in press
Pagano, I., Linsky, J.L., Carkner, L., Robinson, R.D., Woodgate, B., Timothy, G.: 2000, ApJ 532, 497
Peres, G., Orlando, S., Reale, F., Rosner, R., Hudson, H.: 2000, ApJ 528, 537
Redfield, S., Linsky, J.L., Ake, T.B., Ayres, T.R., Dupree, A.K., Robinson, R.D., Wood, B.E., Young, P.R.: 2002a, submitted to ApJ
Redfield, S., Linsky, J.L., Ake, T.B., Ayres, T.R., Dupree, A.K., Robinson, R.D., Wood, B.E., Young, P.R.: 2002b, in preparation
Robinson, R.D., Linsky, J.L., Woodgate, B.E., Timothy, J.G.: 2001, ApJ 554, 368
Saar, S.H.: 1993, in: D. Rabin, J. Jeffries (eds.), *Infrared Solar Physics*, IAU Symp. 154, Kluwer, Dordrecht, p. 493